

The Effect of Wellbore Centralization in Geothermal Wells

Michael F. Mendez Restrepo, Adonis Ichim, Catalin Teodoriu

Mewbourne School of Petroleum and Geological Engineering, University of Oklahoma

100 Boyd St, Norman, OK 73069, Norman, OK, USA

Michael.mendez@ou.edu

Keywords: Centralizers, Finite Element Analysis, Wellbore Integrity, Geothermal Energy.

ABSTRACT

Geothermal and hydrocarbons well construction is similar, although the primer may experience higher loads. Several papers have documented failures within the cement layer but some situations remain unclear. The cement layer is used as a mechanical and hydraulic barrier to support the casing and to prevent vertical and horizontal fluid migration. However, the main role of the cement is to create a seal for fluid movement behind the casing. Therefore, the wellbore cementing operation represents one of the most important steps while drilling for geothermal resources or oil and gas.

From a cementing perspective, long-term wellbore integrity strongly depends on the quality of the cementing job, cement slurry formulation, as well as the annular clearance between casing and formation - usually called standoff. With the advancements of Enhanced Geothermal Systems and the use of modern technology enabling directional drilling and formation permeability increase (via hydraulic stimulation), new challenges are encountered throughout the construction phase of geothermal wells. Cementing directional wells is more difficult because of increased frictional pressure losses when circulating the slurry, difficulties while running casing in hole and improper centralization.

This paper handles different scenarios covering effects of temperature increase and different standoff percentages at a constant casing inside pressure through a Finite Element approach. The modeling covers the casing and cement interaction as a function of standoff. We have been able to demonstrate that the lack of centralization, coupled with the increase in the produced fluid temperature, may increase the stress on cement by up to 25% which could aid in understanding some reported failures in geothermal wells.

1. INTRODUCTION

Oil and gas drilling and production is a complex process facing technical, commercial, environmental and social challenges. The exploitation of geothermal resources faces many of these challenges as well. Geosciences, drilling and completions, reservoir and production engineering represent important know-how for both geothermal and petroleum engineering, and become more critical in high temperature applications (Falcone et al., 2015). Therefore, the energy industry should strive and enhance the synergy between these two sectors and improve the technology transfer (Falcone and Teodoriu, 2008).

The concept of technology transfers from the oil and gas sector to the geothermal sector dates back several years ago, but perhaps it has not been as efficient as one would expect. This has been mainly due to different economics between geothermal and hydrocarbon projects, with a longer period of debt service before cost recovery for geothermal exploitation (Falcone et al., 2015). Wellbore integrity, for example, is an important concept in the oil and gas industry which strongly impacts the geothermal industry as well. It ensures the safe transport of fluids from the subsurface to the surface facilities without detrimental effects to the environment through careful planning and material selection. Lack or loss of well integrity can lead to accidents, lost time, and additional costs, making the diagnosis and prevention of the casing-cement-formation system critical. There are several causes that could lead to wellbore integrity issues. These are present in two phases of the well integrity cycle: pre-production (drilling and completion) and production (Carey, 2010). Since the wellbore casing comes in contact with fluid, mechanical cement stresses are commonly induced by pressure and temperature changes in the wellbore due to fluid production, completion and workover operations, and drilling, because the casing is restrained by the cement and cannot move axially or radially. Geothermal wells produce large volumes of high temperature fluids reaching temperatures up to 500 °F (260 °C). These high temperatures reduce the casing steel strength, and through heat transfer impact the properties of the cement sheath. De Andrade et al (2015) demonstrated how the properties of the cement change through the life cycle of the well due to thermal cycling.

Most of the geothermal wells drilling problems may be solved using latest technologies, but well integrity problems might often arise during the production phase. While cementing a well, during the annular cement slurry displacement, some drilling fluids can be left behind, generating voids or channels in the cement sheath, which turns into early cement failure (Ichim et al., 2017). These are more common where the annular clearance between the casing and the wellbore is lower, making good casing centralization an important parameter for mud removal.

The use of centralizers seems to date back to the 1940s and recent technological advancements allows their use in complex directional and horizontal wells. There are more than four types of centralizers available in the oil and gas industry. Rotating bow spring centralizers are the most popular for vertical and slightly deviated wells, available for all casing sizes. Blade helical and solid body

centralizers are most common in highly deviated and horizontal wells. Here, the contact area is lower, reducing the drag forces present when the casing is run into the wellbore.

Because of its importance to the drilling and production phase of a safe and cost-efficient geothermal well, this paper analyzes the effect of centralizer placement on wellbore stresses and points out the future need for research to improve the prediction of loads generated by standoff and temperature.

2. THE ANALYTICAL MODELS AND PARAMETERS

The interaction between casing, cement, and formation strongly influence the integrity of a wellbore, and makes the understanding of the mechanical properties of all wellbore components vital. The long-term wellbore integrity depends on the eccentricity of the casing in the wellbore and the annular clearance between casing and formation - usually called standoff - with 100% standoff when the casing and the wellbore are concentric, and 0% standoff when the casing touches the borehole or the previous casing (see **Fig. 1(a)**). The eccentricity of the wellbore mainly depends on the forces around the casing, such as material weight and applied tension or compression. Therefore, the casing will be in different positions throughout the wellbore trajectory, as shown in **Fig.1 (b)**.

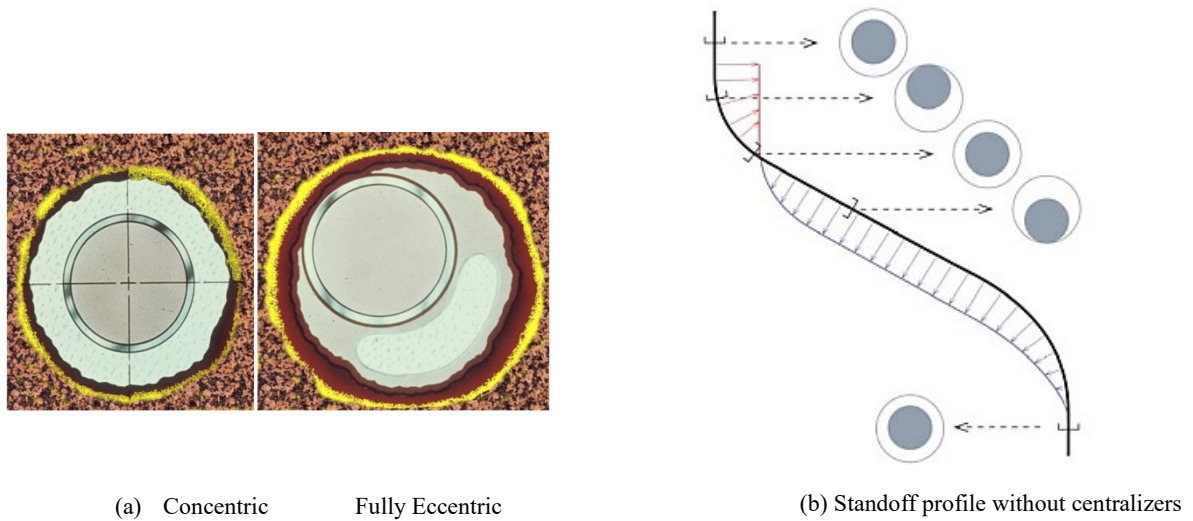


Figure. 1 Wellbore eccentricity and casing standoff (Farley and Scot, 2011; Liu and Weber, 2012)

Casing centralization in the wellbore or in another casing string is usually expressed as percentage standoff (%). This is calculated as $Standoff = C / (A - B) * 100$, where C is the shortest distance between the pipe wall and the wellbore, A is the hole diameter and B the pipe outer diameter, expressed in units of length (**Fig. 2**).

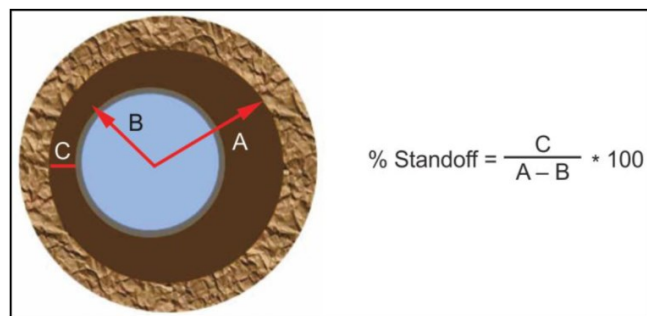


Figure. 2 Standoff ratio (Fry and Pruett, 2015)

In order to demonstrate the importance of appropriate standoff on casing and cement stress development, a finite element analysis (FEA) study was performed in a 2D model by using the plane strain function of ANSYS R16.2. A segment of a vertical well of unit thickness was built in a two-dimensional plain strain element, since the cement, casing and formation are constrained axially at both ends and the casing internal pressure is uniform. Strain components ϵ_z, γ_{xz} and γ_{yz} are zero. Rock overburden and formation pressure will not be considered, since the element thickness is small when compared to the well total length. Minimum and maximum horizontal stresses are not considered. Also, we assume an undeveloped and low geo-stress formation. The finite element model for a concentric case is shown in **Fig. 3a** and the fully eccentric case is shown in **Fig. 3b**.

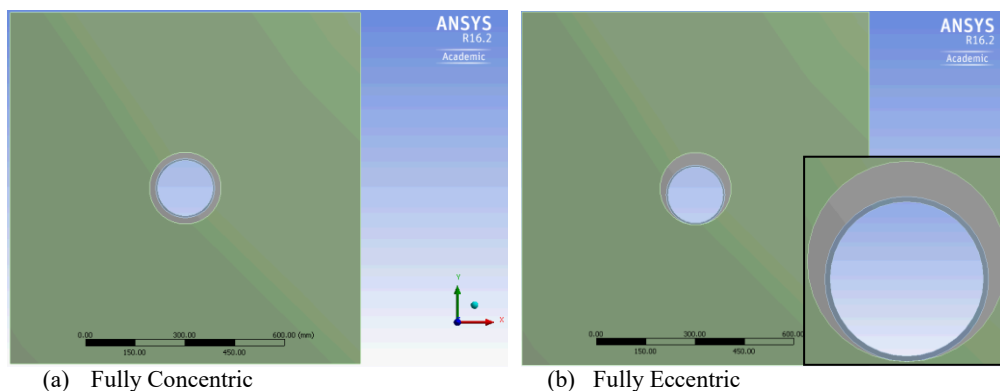


Figure. 3 Finite element model for standoff vs maximum stress analysis.

For an accurate depiction of the influence of standoff on casing and cement stresses, seven different standoff cases were modeled as shown in Table 1. Figure 4 shows the physical model for a 100 %, 67% and 1 % standoff. The 67% standoff was modeled because the mechanical properties of centralizers are tested to a minimum standoff of 67% according to the American Petroleum Institute (API) Specification 10D. This is the lowest value accepted by the API 10D specification and should be regarded as a minimum recommendation to ensure that the centralizer is not efficient.

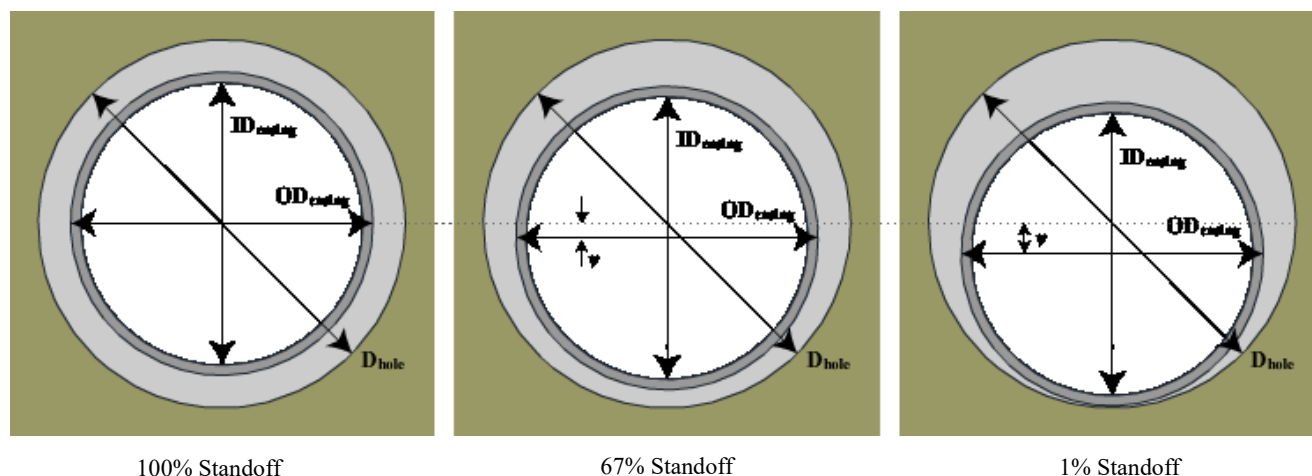


Fig. 4 Three cases used for finite element analysis

Table 1. Geometry used for finite element analysis cases

Case	100% Standoff	80% Standoff	67% Standoff	60% Standoff	40% Standoff	20% Standoff	1% Standoff
Casing offset from hole center, v (in.)	0	0.15	0.24375	0.3	0.45	0.6	0.7425

For all the seven cases, the borehole outer diameter was 8.5 in. (216 mm) and the cement layer inner diameter was 7 in. (178 mm), equal to the casing outer diameter. The casing inner diameter is 6.538 in. (166 mm), and its wall thickness is 0.462 in. (11.7 mm). The casing offset from the hole center (v in Figure 4, expressed in inches) corresponds to the percent standoff and is used in the sketch to ensure accuracy. 0% standoff is not possible to be modeled since this would lead to an intersection of the two faces. The formation boundary was a 33" by 33" (838 mm x 838 mm) square with a size more than fivefold the size of the borehole, in order to avoid the influence of boundary effects on stress. The same mesh grid was used for all of the components. All the elements in the mesh were converted from squares to triangles allowing a better transition among different sizes. Also, a mesh refinement was applied to the casing and cement because the size of these elements is smaller and they find themselves in the vicinity of the force exerted by the fluid pressure, theoretically leading to a stress accumulation. The computational time for each case was between 4 and 5 minutes.

Table 2 shows the material properties for the three components. This information was obtained from experimental work found in the literature (Teodoriu et al., 2015; Yan et al., 2016). The casing, cement and formation are assumed to have an isotropic elasticity. It is also assumed that deformation obeys the pure elastic model.

Table 2. Material Properties

Material	Elastic modulus	Poisson's Ratio	Density
	GPa	-	kg/m ³
Casing	200	0.2	7850
Cement	12	0.3	1800
Formation	8.5	0.2	2250

For boundary conditions, an internal pressure of 5,000 psi (34.5 MPa) was applied uniformly over the casing interior face. An external fixed support was set up over the formation outer edge to resemble the rest of the rock formation, and frictionless supports were added to the two casing, cement and formation faces in order to keep them free regarding in-plane displacements (translational/rotational) whereas displacements normal to the plane are fixed.

Considering that geothermal wells exhibit high temperatures during production, which theoretically decrease the strength of the casing and increases the stresses around the casing, three different cases were analyzed at constant pressure: temperature of 22 °C (set as default in the FE software), 100 °C and 200 °C. The temperatures were applied directly to the casing interior.

3. RESULTS

The following equivalent (von Mises) stresses distributions for the three cases were obtained. Based on the above mentioned, only the diagrams for 100%, 67%, 1% will be shown in what follows. The plots of maximum stress versus standoff include the results of all seven standoffs evaluated. The von Mises equation calculates the net energy stored by element distortion, and outputs the value as an equivalent stress. Maximum stresses are observed on the casing steel for all the cases.

3.1. Case 1: Applied temperature of 22 °C

A maximum stress of 315.3 MPa occurs at 100% standoff, and a maximum stress of 333.3 MPa occurs at 1% standoff. There is an increase of almost 6% from the best to the worst centralization. The orientation of the maximum stresses also changes with a standoff decrease, a shift being observed toward the lower part of the casing. An explanation is the lack of cement sheath at that specific point, and thus, closer contact with formation. For this model, formation has a higher density and a lower Poisson’s Ratio, which constrains more casing expansion, increasing stress. On the other hand, the minimum stress changes insignificantly.

For all the standoff evaluated, a maximum cement stress around 23 MPa was observed with a variation of less than 1 MPa. However, a steep stress changes of approximately 8 MPa occurs in the cement within a short distance for the worst centralization (Fig.6). The slope of the graph for lower standoff values becomes higher, which means that the maximum stress variations increase more when the centralization is worse.

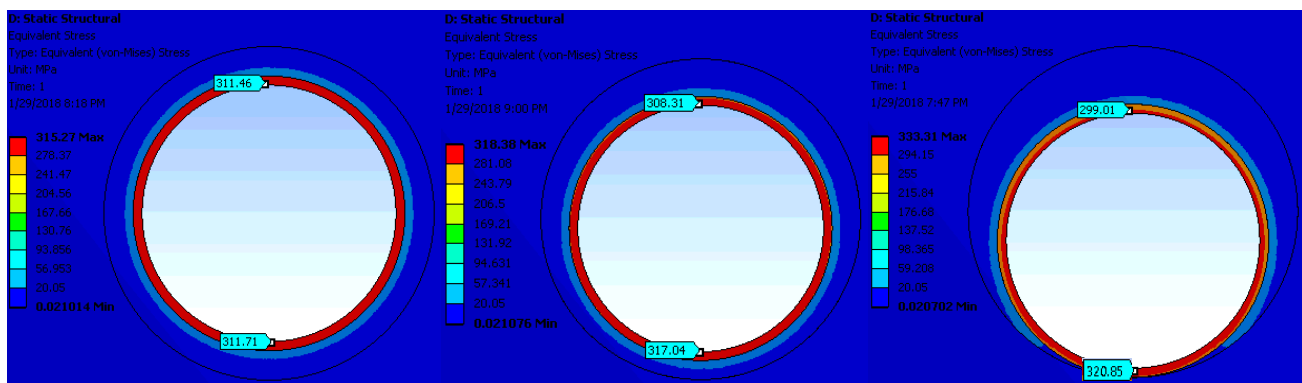


Figure 5. Stress distribution with 100% standoff (left), 67% standoff (center), and 1% standoff (right) at 22°C

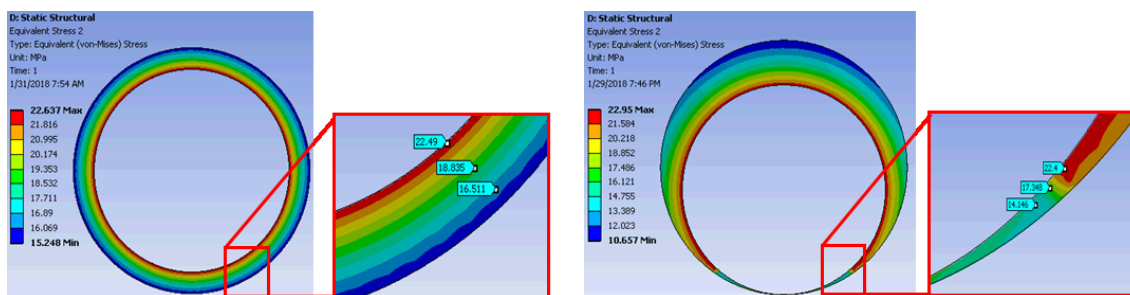


Figure 6. Stress distribution in the cement sheath for 100% left 1% standoff (right)

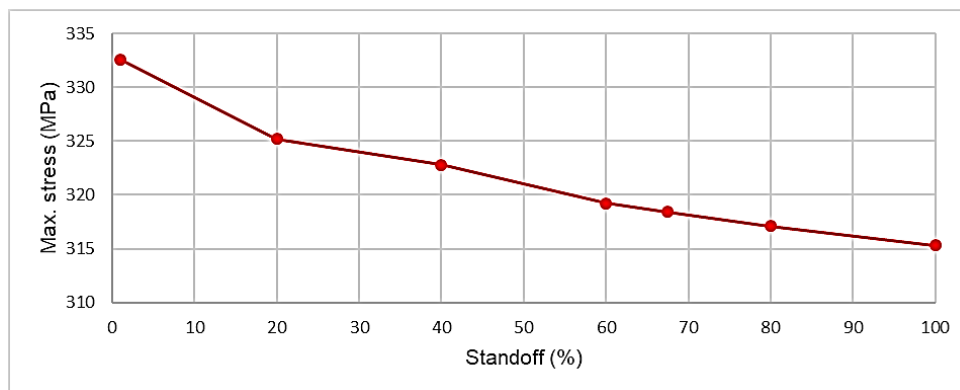


Figure 7. Maximum stress at different standoff for a differential temperature of 22 °C.

3.2. Case 2: Casing temperature of 100 °C ($\Delta T=78^\circ\text{C}$)

A maximum stress of 314.1 MPa occurs at 100% standoff, and a maximum stress of 335.8 MPa is observed at 1% standoff. There is an increase of 7% from the best to the worst case. Again, the orientation of the maximum stresses also changes with a standoff decrease, a shift toward the lower part of the casing being observed. The results of maximum and minimum stresses on the casing steel are similar to what is observed in Case 1. For all the standoff evaluated, a maximum cement stress around 35.6 MPa was observed with a variation of less than 1 MPa, which is 57% higher than the previous case evaluated. Again, a representative stress difference is present for the worst centralization with a higher value of 11 MPa, as shown in Fig. 9). For this case, a stress higher than 20 MPa occurs over the entire cement layer, also noticed in the formation for the lower standoff values. Likewise, the slope of the graph for lower standoff values becomes higher, but in this case, the maximum stress variations increase even more with worse centralization.

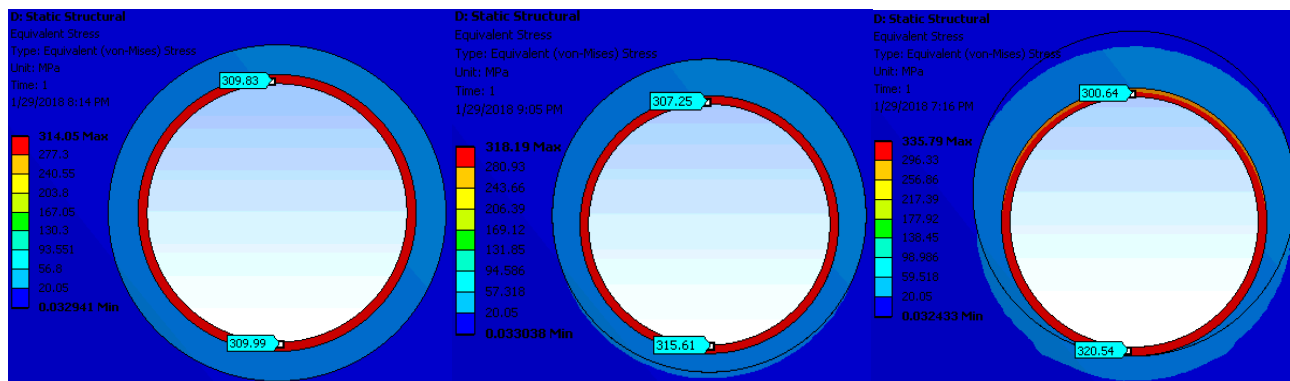


Figure 8. Stress distribution with 100% standoff (left), 67% standoff (center), and 1% standoff (right) at 100°C

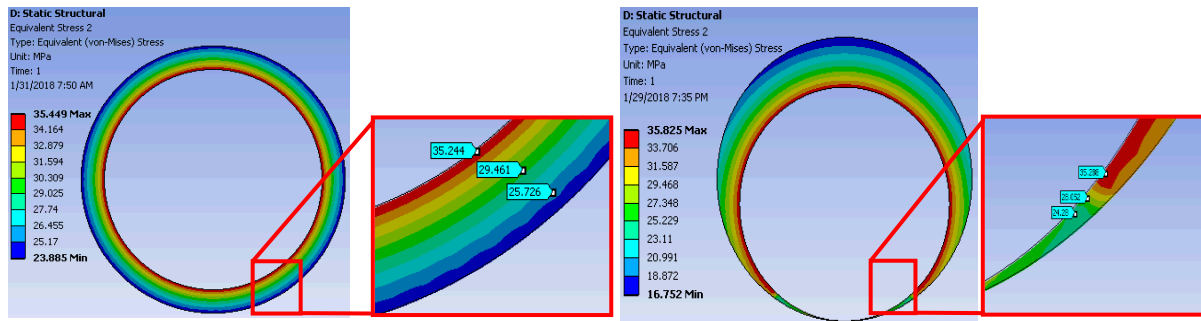


Figure 9. Stress distribution in the cement sheath for 100% left and for 1% standoff (right) at 100°C

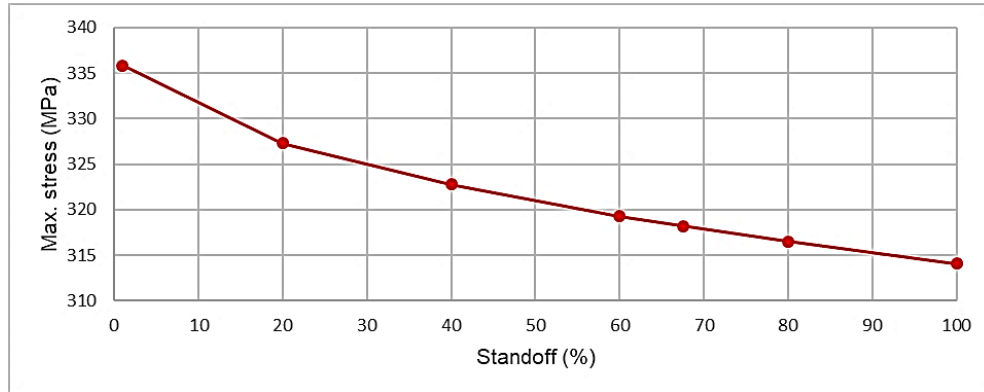


Figure 10. Maximum stress at different standoff for a differential temperature of 100 °C.

3.3. Case 3: Casing temperature of 200 °C ($\Delta T=178^\circ\text{C}$)

A maximum stress of 449.9 MPa occurs at 100% standoff, and a maximum stress of 469.1 MPa occurs at 1% standoff. There is a maximum equivalent stress increase of almost 5% from the best to the worst centralization. Interestingly, the orientation of the maximum stresses does not change with a standoff decrease for this case. The results of maximum stress on the casing steel are much higher than the cases of 22°C and 100°C shown above, with an increase of 43% compared with the case 1. Minimum stress is also higher.

For all the standoff evaluated, a maximum cement stress of approximately 52 MPa was observed with a variation of less than 1 MPa, and it increased 48% when compared to case 1. Like in the two previous cases, a representative cement stress difference is present for the worst centralization with a value of 19 MPa (Fig. 12). For this temperature, a stress higher than 20 MPa occurs over the cement sheath and the formation for all the centralization cases. The slope of the graph for lower standoff values also becomes higher, and in this case the maximum stress variations increases even more than in the previous cases when the centralization is worse.

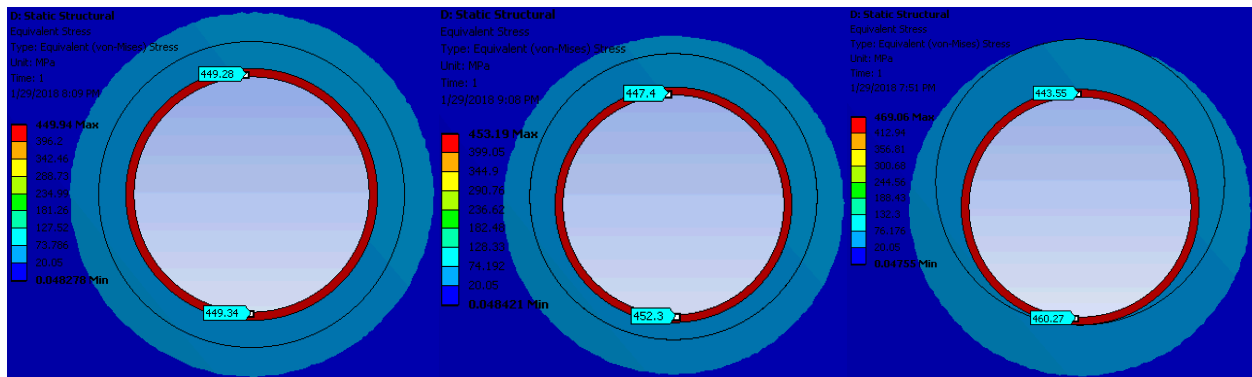


Figure 11. Stress distribution with 100% standoff (left), 67% standoff (center), and 1% standoff (right) at 200°C

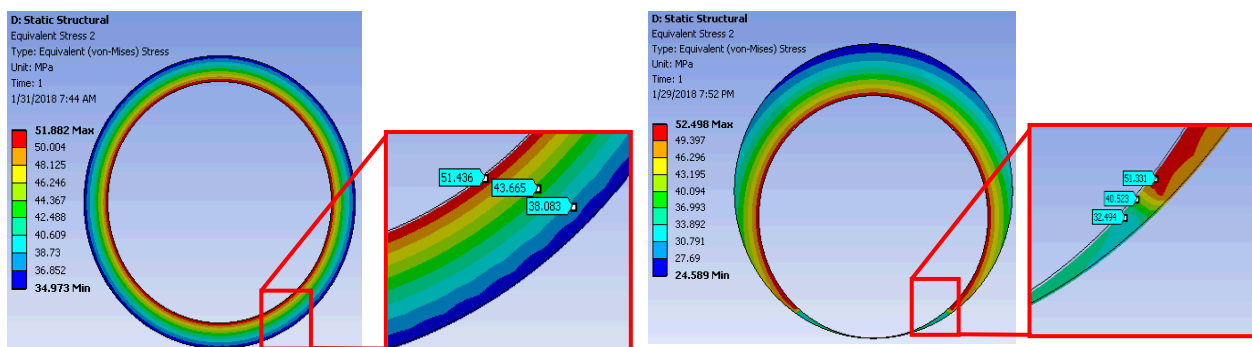


Figure 12. Stress distribution in the cement sheath for 100% left and for 1% standoff (right) at 200°C

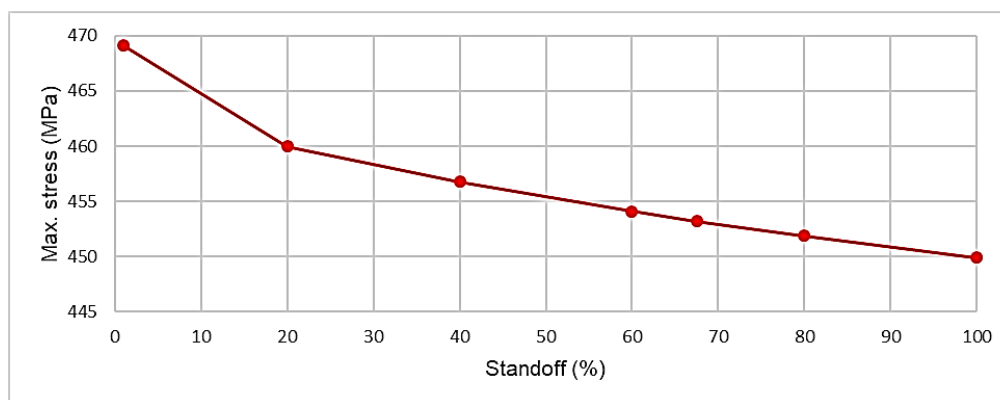


Figure 13. Maximum stress at different standoff for a differential temperature of 200 °C.

4. DISCUSSIONS

The simulations presented above show that the combination of poor standoff and high differential temperature may induce additional stresses in casing and the cement sheath. By comparing Figure 7 with Figure 13, it can be observed that the maximum stress in case of casing-wellbore contact (1% standoff) will lead to a stress increase inside of the casing wall of almost 140 MPa, which represents a 42% increase for 1% standoff. Within the same temperature range, the stress increase due to changes in standoff is 30 MPa, approximately 7% increase when compared to values for 100% standoff. Although the stress increase might seem small, it is worth mentioning that some design factors (such as burst) are only 10% above 1 (API design factor for burst is 1.1). The calculated stress induced by internal pressure through the API equation for maximum yield pressure is 295 MPa, but if we relate the maximum stress obtained for case three to it, the stress change is almost 35%, which is beyond the typical design factor

The cement stresses show a higher increase when temperature is changed. The maximum equivalent stress in the cement is changing from 22.4 MPa (in Cases 1) to 51.8 MPa (Case 3), an increase of 131%.

A study performed by Ichim, Marquez and Teodoriu (2016) reveal that cements cured for extended time periods (110 days curing time) that are exposed to temperature cycles show a decrease of their unconfined compressive strength of up to 25% after 12 thermal cycles. In their work, the measured samples (mixed without additives) exhibited a decrease from 75 MPa to about 60 MPa in their unconfined compressive strength after exposure to temperature cycles of 80°C (Figure 14). However, a 60 MPa UCS for cements used in high temperature application could not be achieved due to the increased number of additives used against cement thermal retrogression.

The increase of maximum stress as a function of standoff exhibits linear behavior between 60 and 100% standoff. This leads to a stress increase of only 1.5% from the 100% standoff for Case 1 to only 1% increase for Case 3, however the magnitude of stress is higher for Case 3. The importance of centralizers becomes visible for the 1% standoff (no centralizer) where stresses are much higher. It is to be noted that we only discuss the importance of centralizers from the mechanical point of view. An additional disadvantage of smaller is poor annular circulation leading to poor or incomplete cementation, which is not discussed in this paper.

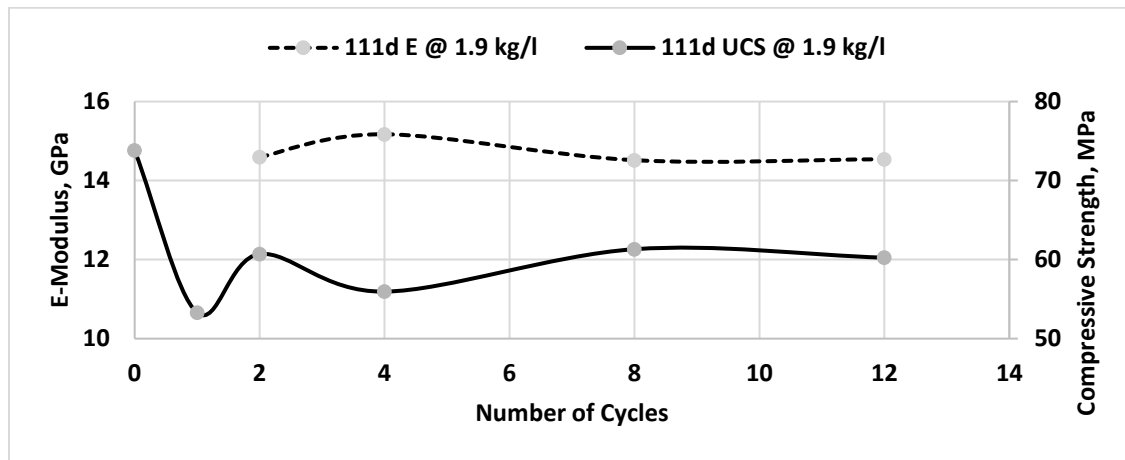


Figure 14. Effect of thermal cycles on class G cement mechanical properties (E-Modulus and UCS) cured for 110 days.

5.CONCLUSIONS

The case of good and bad centralization has been simulated in this work, using a vertical well as synthetic case. The case of not using centralizer is represented by a standoff of 1%, mainly because of the limitations in the finite element modeling.

Through finite element analysis, the effects of casing centralization and casing inside temperature on wellbore stresses have been analyzed. We found out that the standoff will affect the stress distribution in casing and cement, increasing the maximum stress in the casing by more than 10% when standoff and applied differential temperature are considered.

The presented simulations have shown a linear dependency between standoff and stress increase in casing, and that a good centralization leads to a reduction of the maximum von Mises stress on casing when the casing is exposed to internal pressure and temperature variation.

REFERENCES

- Bourgoyne, P.: "Applied Drilling Engineering", Society of Petroleum Engineering (1991)
- De Andrade, J., Sangesland, S., Todorovic, J., Vrålstad, T.: Cement Sheath Integrity During Thermal Cycling: A Novel Approach for Experimental Tests of Cement Systems, SPE-173871-MS, SPE Bergen One Day Seminar, Bergen, Norway (2015)
- Falcone, G., Pawellek, C. and Teodoriu, C.: The First Master in Geothermal Engineering Offered by a Petroleum Engineering School: Curriculum Challenges and Opportunities, SPE-176746-MS, SPE Annual Technical Conference and Exhibition, Houston, (2015).
- Falcone, G. and Teodoriu C.: Oil and Gas expertise for Geothermal Exploitation: The Need for Technology Transfer, SPE 113852, EAGE/SPE EUROPEC Conference, Rome, (2008)
- Ichim, A., and Teodoriu, C.: Revisiting Thermal Well Integrity through a Closer Look at Casing-Cement-Formation Interaction. SPE-182525-MS, SPE Thermal Well Integrity & Design Symposium, Banff, Alberta, Canada (2016).
- Ichim, A. C., Marquez, A., and Teodoriu, C. How Accurate is Your Well Integrity? A Discussion About the Surface Casing Integrity Under Temperature Loading in Heavy Oil Fields, SPE-181154-MS, SPE Latin America and Caribbean Heavy and Extra Heavy Oil Conference, Lima, Peru, (2016).
- Wehling, P.: "Wellbore Cement Integrity Testing", Master's Thesis, TU-Clausthal, (2008)
- Yan, W., Deng, J., Ge, H., Zou, L., Li, H., Wang, H.: Investigation of Casing Deformation During Hydraulic Fracturing in High Geostress Shale Gas Play Journal of Petroleum Science and Engineering, (2016).
- Farley, D. B., and Scott, T. J.: Field Proven Solutions to the Challenges of Centralizing Solid Expandable Casing. SPE-146507-MS, SPE Annual Technical Conference and Exhibition, Denver, CO 46507-MS (2011)
- Fry, D., and Pruet, B.: An Analytical Comparison of Wellbore Deviation and its Effects on Proper Centralization in the Bakken. SPE-174064-MS, SPE Western Regional Meeting, Garden Grove, CA, (2015)
- Liu, G., and Weber, L. D.: Centralizer Selection and Placement Optimization. SPE-150345-MS, SPE Deepwater Drilling and Completions, Galveston, TX, (2012)